On the design of a computational simulator for turbulent turbidity currents

Zio Souleymane[1], Henrique F. da Costa[1], , Gabriel M. Guerra[1]
Fernando A. Rochinha[1] , Paulo Paraizo[2]
Jose J. Camata[3], Renato N. Elias[3], Alvaro L. G. A. Coutinho[3]

[1]Mechanical Engineering Department, Federal University of Rio de Janeiro
[2]Petrobras UO-SEAL Sergipe Operational Unity, Aracaju, Sergipe
[3]High Performance Computing Center,Federal University of Rio de Janeiro

July 10, 2018

Outiline

- Background and Motivation
- Introduction
- Mathematical Modelling of Turbidity Currents
- Computational Simulation
- Uncertain Rheology of Non Dilute Currents
- Numerical Computations
- Final Remarks

Background and Motivation

- Particle-laden flows are responsible for carrying sediments with organic matter leading to formations hosting oil reservoirs.
- A large amount of Brazilian oil reservoirs (indeed worldwide) were formed by the action of **Turbidity Currents**.
- Sediments carried by turbidity currents (turbidites), encompasses a family of deposits with some common characteristics. The geometries and grain sizes of the deposits can vary due to complex interactions between current dynamics, seafloor irregularities, slope and sediment supply
- Modeling and simulating this process can help to understand what controls the deposits, what, in turn, can help policy makers to come up with more robust and efficient decisions.

Turbidity Current: What is?

It is a downhill flow of water due to increased density caused by sediments[1]

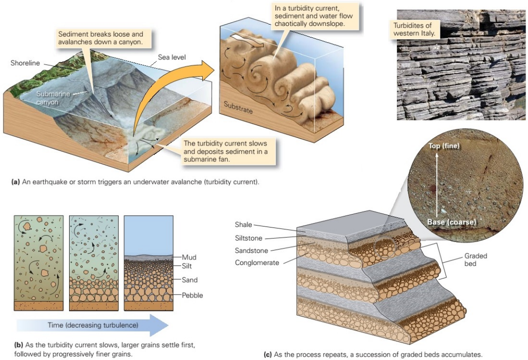

(a) An earthquake or storm triggers an underwater avalanche (turbidity current).

(b) As the turbidity current slows, larger grains settle first, followed by progressively finer grains.

(c) As the process repeats, a succession of graded beds accumulates.

Turbidity currents can change the physical shape of the sea floor by eroding large areas, creating underwater geological formations with oil and gas reservoirs. According to Meiburg & Kneller, $Re = \mathcal{O}(10^9)$ in nature.
a huge amounts of sediments usually in a gradient pattern, with the largest particles at the bottom and the smallest ones on top.

[1] Sedimentary structures by Owais Khattak http://geologylearn.blogspot.com.br/2015/11/sedimentary-structures.html

What we see today and what we're trying to reconstruct: seismic as primary data but it needs more...

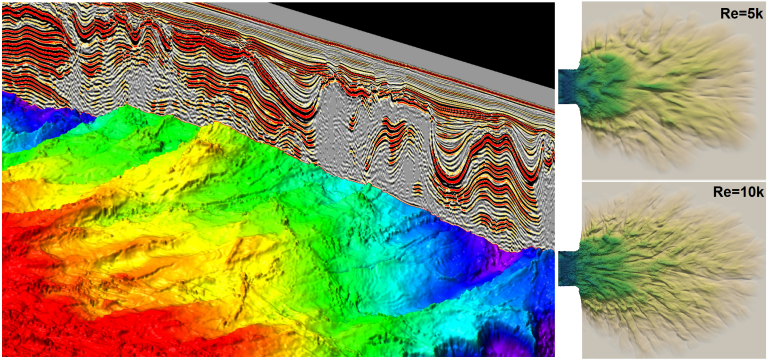

Figure: : 3D seismic survey [1]; : Computed Deposition for Re=5K , 10K

[1]CGG Veritas Data Library, http://www.cgg.com/

Polidysperse Particle Laden Flows

Governing equations:

Fluid: Incompressible Navier Stokes

$$\rho \left(\frac{\partial \mathbf{u}}{\partial t} + \mathbf{u}.\nabla \mathbf{u} \right) = \nabla \cdot (-p\,\mathbf{I} + \mu(c_i)\,\nabla \mathbf{u}) + \mathbf{e}^g \sum_{i=1}^{N} c_i = 0$$

$$\nabla \cdot \mathbf{u} = 0$$

Sediment Transport: advection–diffusion

$$\frac{\partial c_i}{\partial t} + (\mathbf{u} - u_{s_i}\mathbf{e}_g) \cdot \nabla c_i = \nabla \cdot (\alpha_i \nabla c_i)\,(i = 1, ..., N)$$

where $\mathbf{u}$, p, t, are non-dimensional velocity, pressure, time, and N the number of sediment sizes. Boundary condition (bottom): sediments deposition, u_b, buoyancy velocity, $\frac{\partial c_i}{\partial t} = u_{s_i} \frac{\partial c_i}{\partial z}$ and initial conditions $c_i(.,0)$, with

$$\alpha_i = \frac{1}{Sc_i \sqrt{Gr_i}} \quad Gr_i = \left(\frac{u_b H}{\nu_i} \right)^2 \quad Sc_i = \frac{\nu_i}{\kappa_i}$$

Deposition Mapping (deposits height and composition)

$$D_i(\mathbf{x}, t) = \int_0^t u_{Si}\; c_i(\mathbf{x}, t)\; d\tau \quad (i = 1, ..., N)$$

Polidysperse Particle Laden Flows: FE Formulation

Fluid: Incompressible Navier Stokes – RB-VMS

$$
\begin{aligned}
&(\rho\frac{\partial \mathbf{u}_h}{\partial t}, \mathbf{w_h}) + \rho(\mathbf{u}_h.\nabla\mathbf{u}_h, \mathbf{w}_h) + 2\mu(c_h + c')(\nabla^s\mathbf{u}_h, \nabla^s\mathbf{w}_h) - (p_h, \nabla.\mathbf{w}_h) \\
&- (c_h\,\mathbf{e}^g, \mathbf{w}_h) + (\nabla.\mathbf{u}_h, q_h) - (\mathbf{w}_h, 2\mu(c_h + c')\nabla^s\mathbf{u}_h) - \sum_{e=1}^{Nel}(\rho(\mathbf{u}', \mathbf{u}_h\nabla.\mathbf{w}_h)_{\Omega_e} \\
&+ (2u'.\nabla\mathbf{w}_h, \nabla\mu(c_h + c'))_{\Omega_e} + (\mathbf{u}', 2\mu(c_h + c')(\mathbf{u}', \Delta\mathbf{w}_h))_{\Omega_e} - (p', \nabla.\mathbf{w}_h) \\
&- (\rho\mathbf{u}', \nabla q_h) + (\rho\mathbf{u}'.\nabla\mathbf{u}_h, \mathbf{w}_h) - (\rho\mathbf{u}', \mathbf{u}'\cdot\nabla\mathbf{w}_h) - (c'\,\mathbf{e}^g, \mathbf{w}_h) = 0
\end{aligned}
$$

Sediment Transport: advection–diffusion

$$
\begin{aligned}
&(\rho\frac{\partial c_h}{\partial t}, \upsilon_h) + (\rho(\mathbf{u}_h + \mathbf{u}' + u_s\mathbf{e}^g)\cdot\nabla c_h, \upsilon_h) + \alpha(\nabla c_h, \nabla\upsilon_h) \\
&- \sum_{e=1}^{Nel}\Big((\rho\mathbf{u}_h.\nabla v_h, c')_{\Omega_e} + (\rho(\mathbf{u}' + u_s\mathbf{e}^g).\nabla v_h, c')_{\Omega_e} + \alpha(c', \Delta\upsilon_h)_{\Omega_e}\Big) \\
&- u_s(\mathbf{e}^g\cdot\mathbf{n})\,(c_h, \upsilon_h)_{\Gamma_h^c} - \frac{1}{u_s}\left(\frac{\partial c_h}{\partial t}, \upsilon_h\right)_{\Gamma^c_{bottom}} + \sum_{e=1}^{Nel}(\delta\,(c_h)\,\nabla\upsilon_h\cdot\nabla c_h)_{\Omega^e} = 0
\end{aligned}
$$

Computational Aspects :EdgeCFD Overview

- **EdgeCFD**[2]: *A general purpose parallel FE CFD solver*
  - Edge-based data structure and Linear Tetrahedra;
  - Hybrid parallel (MPI, OpenMP or both);
  - SUPS+LSIC and RB-VMS FE formulation for incompressible flow;
  - ILES turbulence treatment;
  - $\mathbf{u}$-p fully coupled flow solver;
  - SUPG/YZβ formulation for transport and compressible flow;
  - Adaptive time step control;
  - Inexact-Newton Krylov solver;
  - Communication-free uniform mesh refinement
- **Modules**:
  - Compressible and Incompressible flows;
  - Fluid-Structure Interaction (FSI/Rigid Body in ALE framework);
  - Free-surface flow (VoF and Level Sets);
  - Multiphase flows

[2] Developed at COPPE for PETROBRAS since 2007

Computational Aspects: EdgeCFD Solver

EdgeCFD Block-Iterative Time Marching Algorithm

Pseudocode for coupled Navier-Stokes -Transport equations

while $t_o < t_f$ **do**

    while $i < i_{max}$ **do**
        Solve Navier-Stokes equations
        Non-linear method: Inexact-Newton Krylov with Backtracking
        Linear solver: Block-diagonal preconditioned GMRES(m)
    end while

    while $j < j_{max}$ **do**
        Solve Transport equations
        Non-linear method: Newton-like (multi-corrector)
        Linear solver: Diagonal preconditioned GMRES(m)
    end while

    if Time step control is activated **then**
        update Δt
    end if
    $t = t + \Delta t$
end while

EdgeCFD Simulation Setup Configuration

Succesive Discharges on NECOD's Experimental Basin Tank

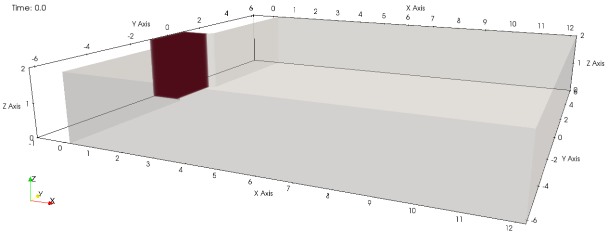

- Lock-Exchange configuration, monodisperse current, three successive discharges
- Dimensions $(x, y, z) = (12, 12, 2)$
- Sediments deposit $(x, y, z) = (2, 1, 2)$
- Initial relative concentration $= 1$, Settling velocity $u_s = 0.02$
- Boundary conditions: no-slip at bottom; no-penetration in all walls; free top
- Simulation time for each discharge: 30 time units with time step 0.01

Tank simulation

Three Successive Discharges

Re = 10000

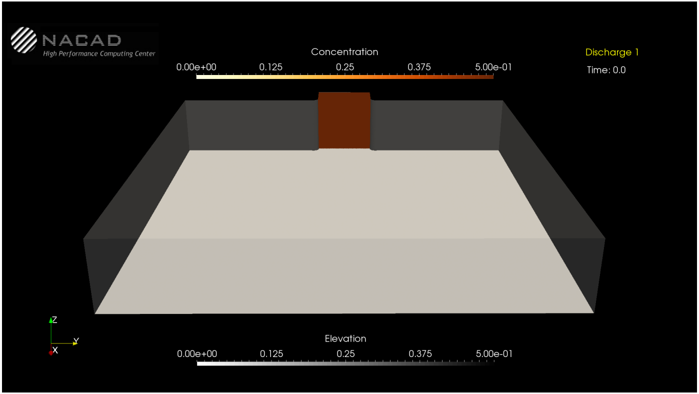

Runs on SGI ICE-X (504 CPUs Intel Xeon E5-2670v3 (Haswell): 6048 Cores) "*Lobo Carneiro*" UFRJ supercomputer

Experimental Channel

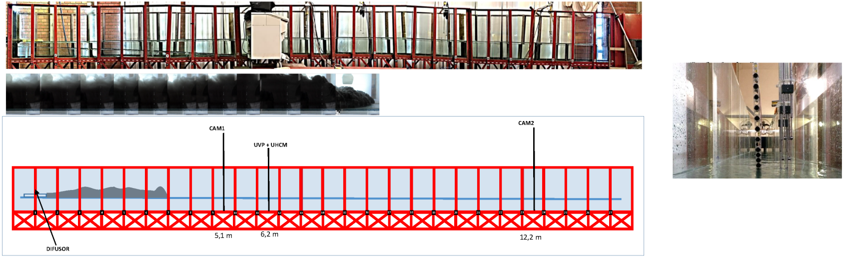

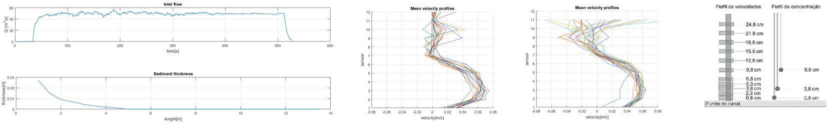

Figure: **Top**: NECOD's Experimental channel set-up and measurement devices; **Bottom**: Measurements

Experimental Channel

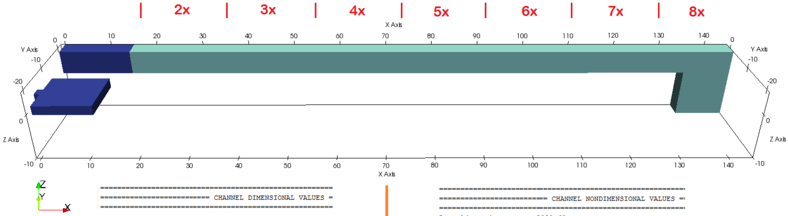


```
==========================================================
========================= CHANNEL DIMENSIONAL VALUES =
==========================================================

Channel lenght                              = 13.50 [m]
Channel width                               = 0.40 [m]
Channel height                              = 0.50 [m]
Tank lenght                                 = 1.00 [m]
Tank width                                  = 0.40 [m]
Tank depth                                  = 1.50 [m]
Inflow height                               = 0.04 [m]
Inflow area                                 = 0.02 [m^2]
==========================================================
Flowrate                                    =   50 [l/min]
Inflow velocity                             = 0.05 [m/s]
Gravity                                     = 9.80 [m/s^2]
Flux height                                 = 0.10 [m]
Specific mass         (ambient fluid) = 1000.00 [kg/m^3]
Kinematic viscosity   (ambient fluid) = 1.00e-06 [m^2/s]
Specific mass              (sediment) = 1191.00 [kg/m^3]
Volumetric concentration   (sediment) = 1.83 [percent]
Sediments diameters                         = 2.7200e-06 [m]
Sedimentation velocity                      = 7.6935e-07 [m/s]
Specific mass of mix                        = 1003.50 [kg/m^3]
Reduced gravity                             = 0.0343 [m/s^2]
Buoyancy velocity                           = 0.0585 [m/s]
==========================================================
```

```
==========================================================
========================= CHANNEL NONDIMENSIONAL VALUES =
==========================================================
Reynolds number      = 5852.69
Froude number        = 1.00
Grashoff number      = 34253940.00
Schmidt number       = 1.00


============================================= Geometry ==
Channel lenght       = 135.00
Channel width        = 4.00
Channel height       = 5.00
Tank lenght          = 10.00
Tank width           = 4.00
Tank depth           = 15.00
Inflow height        = 0.40


======================================== EdgeCFD Inputs =
          viscocity  = 1.7086e-04
                  k  = 1.7086e-04
     velocity_inlet  = 8.8990e-01
settling velocities  = 1.3145e-05
==========================================================
```

Figure: **Top**: Channel and tank domains; **Bottom Left**: Simulation data

EdgeCFD Results Experimental Channel

Setup: (light grey volume), x=3m, y=0.4m, z=0.5m,
elements=44,798,907 tet4
nodes = 7,922,727
walltime = 86h, 144 cores

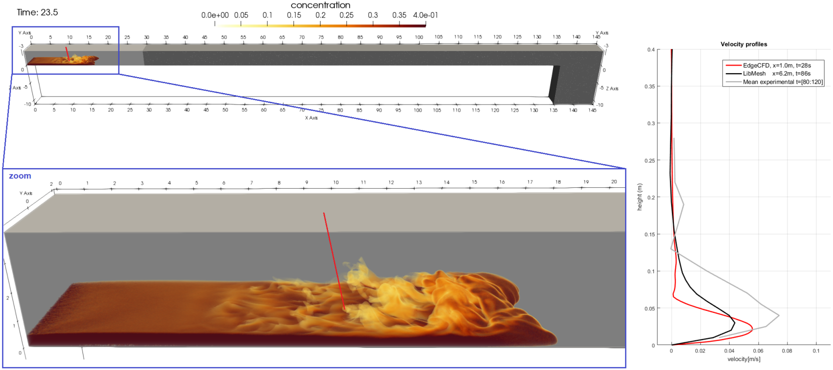

Figure: **Left**: Channel concentration with zoom; **Right**: Velocity profiles

Uncertain Rheology of Non–Dilute Currents

- Complex underlying physics: non-Boussinesq and non-Newtonian behavior, particle-particle interaction.
- In the present context, two-phase flows models are computer intensive.
- One phase-flow employing **rheological laws** for the rheology of the mixture can provide a good balance between computational costs and predictive capabilities.
- For instance, consider **Krieger and Dougherty (1959)** [1] equation for viscosity of suspensions, a pseudo-Newtonian fluid with a sediment concentration dependent viscosity:

$$\mu_m(c) = \mu_f \left(1 - \frac{c}{c_m}\right)^{-\lambda * c_m} \qquad \lambda = 2.6 \quad c_m = 0.744$$

[1] KRIEGER I., AND DOUGHERTY, T. Concentration dependence of the viscosity of suspensions. Trans. Soc. Rheol. 3 (1959), 137–152

Discrepancy: Phenomenological Models

Literature presents a number of well designed and calibrated phenomenological models (standard rheometer tests)

Einstein (1906)	$\mu_m = \mu_f\,(1 + 2.5c)$
Mooney (1951)	$\mu_m = \mu_f \left[\exp\left(\frac{2.5c}{1-\frac{c}{c_m}}\right)\right]$
Krieger and Dougherty (1959)	$\mu_m = \mu_f \left[1 - \frac{c}{c_m}\right]^{-2.5c_m}$; $c_m = 0.74$
Batchelor (1977)	$\mu_m = \mu_f \left[1 + 2.5c + 6.2c^2\right]$
Brady (1993)	$\mu_m = 1.3\mu_f \left[1 - \frac{c}{c_m}\right]^{-2.0}$
Toda and Hisamoto (2006)	$\mu_m = \mu_f \left[\frac{1-0.5c}{(1-c)^3}\right]$
Toda and Hisamoto with k (2006)	$\mu_m = \mu_f \left[\frac{1+0.5kc-c^2}{(1-kc)^2(1-c)}\right]$; $k = 1 + 0.6c$

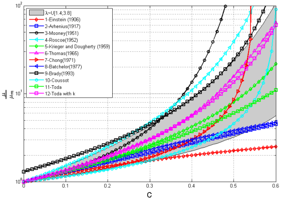

- Grey area - uncertainty in the predictions
- Diversity suggests that, for higher concentrations, the viscosity might depend on other characteristics of the flow

Model Discrepancy: An Excursion into Closure Models

Physical reasoning: What would be the effect in the model response if we consider one phenomenological law trying to cope with the diversity exposed by the set of plausible viscosity models?

Thus, model discrepancy (error) is embbeded[3] in the rheology submodel trhough $\lambda(c, p, \mathbf{u})$ a random uncertain field (physical constraints and observed trends can be enforced) :

$$\mu_m = \mu_f \left(1 - \frac{c}{c_m}\right)^{-\lambda c_m}$$

A first (simple) "by hand" model : $c_m = 0.74$ and $\lambda = \overline{\lambda} + \sigma_\lambda \xi$, where ξ is an independent uniform random variable with support [-1,1]. Moreover $\overline{\lambda} = 2.6$, $\sigma_\lambda = 1.2$. i.e. λ varying in the interval [1.4, 3.8]. That "covers the grey area" (reproduces trends and enforces physical constraints)

[3] Sargysan K. et al. On the Statistical Calibration of Physical Models. Int. J. Chem. Kinetics. 47 (4), 2015

Numerical Results: Forward UQ analysis and Calibration

Computational Setup: closed channel with sustained current

- Channel dimensions, $xc = 6$, $yc = 0.4$, $zc = 0.5$, inlet windows $yw = 0.4$ $zw = 0.04$. Computational setup inspired on a experimental one (calibration and validation)
- Initial relative concentration $= 0.11$ (normalization constant)
- Reynolds number $Re = 1.5x10^4$, used to allow the formation of turbulent structures. Transient flow features.
- No-slip and no-penetration in all walls with inflow velocity $= 0.5$

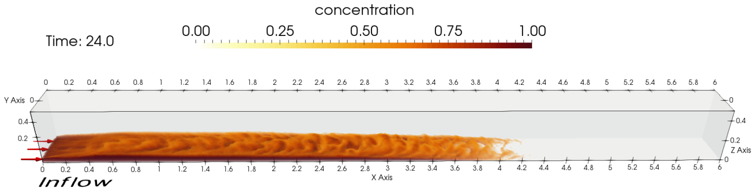

- Mesh, 1.064.311 linear tetrahedra, 212.471 nodes, time step 10^{-2}, simulation time: 24 time units.

Channel simulation

Sustained inlet current

Re = 8000

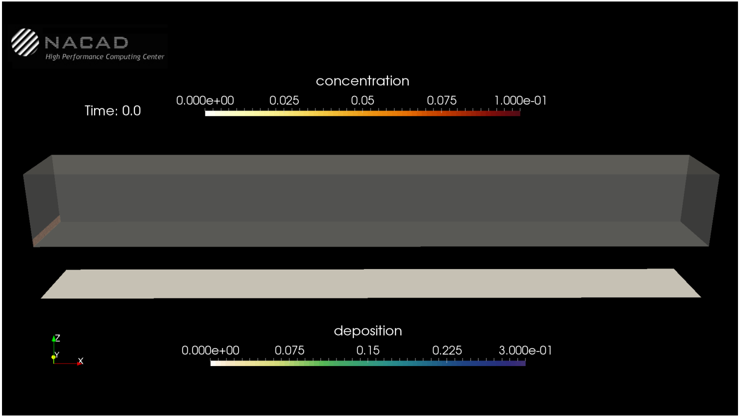

Runs on SGI ICE-X (504 CPUs Intel Xeon E5-2670v3 (Haswell): 6048 Cores) "*Lobo Carneiro*" UFRJ supercomputer

Computational Reliability: mass conservation and energy budget

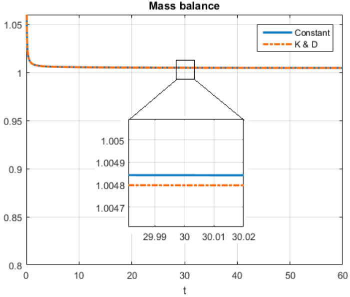

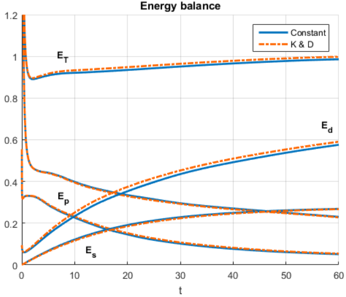

Effects of phenomenological KD viscosity law

Isosurfaces of Q-Criterion colored by vorticity

Re = 8000

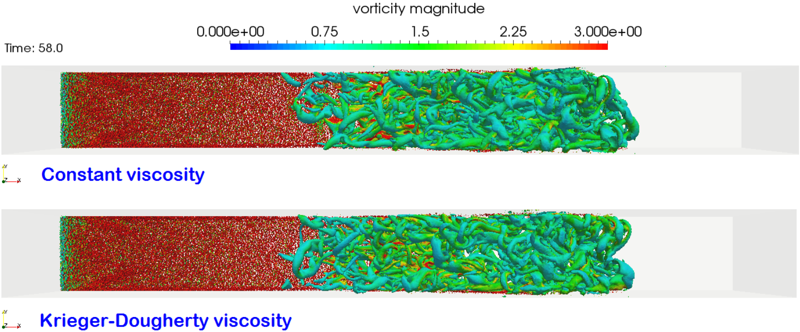

Effects of phenomenological KD viscosity law

Bottom shear stress

Re = 8000

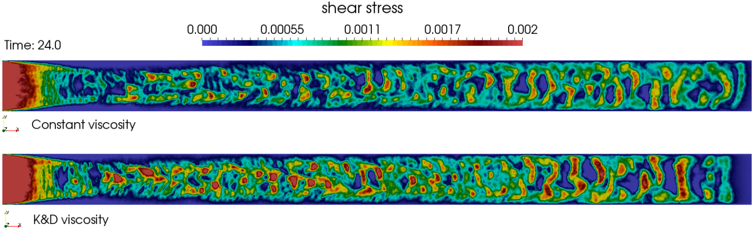

Effects of phenomenological KD viscosity law

Isosurfaces of Q-Criterion colored by vorticity

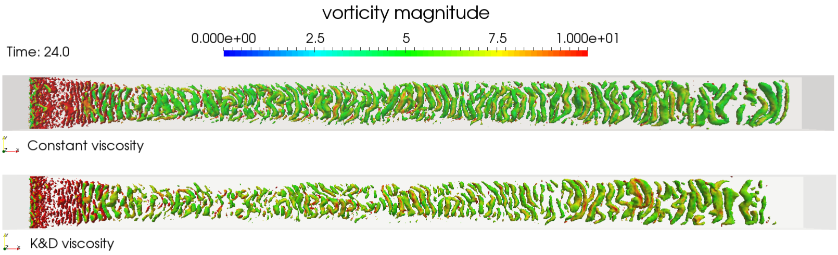

Forward Analysis: uncertainties carried by the current

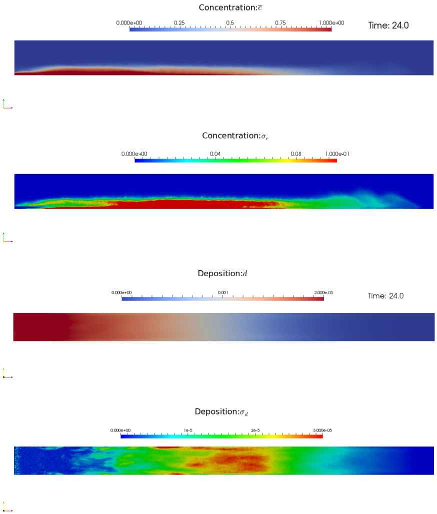

Forward UQ : sensitivity analysis and building a fast surrogate

Embedded model error: Bayesian calibration

- Predictive model:

$$\mathbf{y} = \underbrace{f(\mathbf{x};\lambda)}_{model} + \underbrace{\mathbf{e}}_{observation\ \ noise}$$

- Embedding the model error in λ results into estimation of Λ pdf
- λ a random parameter following a uniform distribution $U(\mu_\Lambda, \sigma_\Lambda)$
- Bayesian formalism leading to parameter estimation of $\alpha = (\mu_\Lambda, \sigma_\Lambda)$

$$\underbrace{P(\alpha \mid \mathcal{D})}_{posterior} \propto \underbrace{P(\mathcal{D} \mid \alpha)}_{likelihood} \underbrace{P(\alpha)}_{prior} \quad (1)$$

Synthethic data $\mathcal{D} = \{y_1, y_2, ..., y_N\}$ **(no observation noise : $\mathbf{e} = \mathbf{0}$)**

$$\mu = \mu_f \left(1 - \frac{c}{c_m}\right)^{-\lambda c_m + t_1 c + t_2}$$

where $t_1 = -0.3$ and $t_2 = 0.2$ (tuned to make the synthetic data compatible with the observations in the literature).

Likelihood: a key issue

- **Full Likelihood**[4]: degenerate ($\mathbf{e} = \mathbf{0}$) and computationally intensive

$$L(\alpha) = \int p(\mathcal{D}|\lambda)\ p(\lambda|\alpha)\ \ d\lambda$$

- **Unconventional likelihoods**
  - Marginalized Gaussian Approximation

$$L(\alpha) = \frac{1}{(2\pi)^{\frac{N}{2}}} \prod_{N}^{i=1} \frac{1}{\sigma_i(\alpha)} \exp(-\frac{(\mu_i(\alpha) - y_i)}{2\sigma_i(\alpha)^2}),$$

  - Aproximate Bayesian Computation (ABC)

$$L(\alpha) = \frac{1}{\epsilon\sqrt{2\pi}} \prod_{i=1}^{N} exp\left(-\frac{(\mu_i\,(\alpha) - D_i)}{2\epsilon^2}\right)$$

$\mu(\alpha; x) = E_\xi[f(x; \lambda(\xi; \alpha))]; \sigma(\alpha; \mathbf{x})^2 = \mathbf{V}_\xi[\mathbf{f}(\mathbf{x}; \lambda(\xi; \alpha))]$, "fast" surrogate.
Priors are designed to enforce physical trends

[4] Sargysan K. et al. On the Statistical Calibration of Physical Models. Int. J. Chem. Kinetics. 47 (4), 2015

Calibration Data and First Results

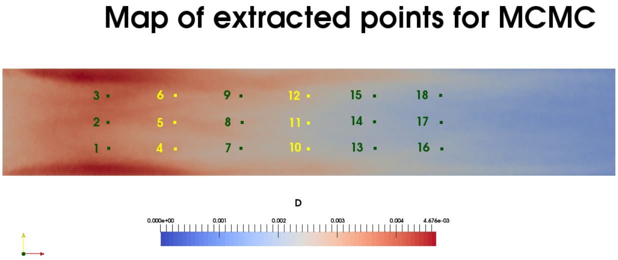

Figure: Bottom view - observation points (heterogeneous sediment deposition (t=24) - yellow calibration points)

Likelihood	Calibration Data	μ_λ	σ_λ
Gaussian Marginalized	6 D	2.32661912	0.572279078
	6 D + 3 V	2.35322742	0.58770447
ABC Mean Only	6 D	2.919928835	0.113485228
	6 D + 3 V	2.60539595	0.134949686
ABC Mean + Std	6 D	2.91597052	0.103799792
	6 D + 3 V	2.12970724	0.10617043

Validation

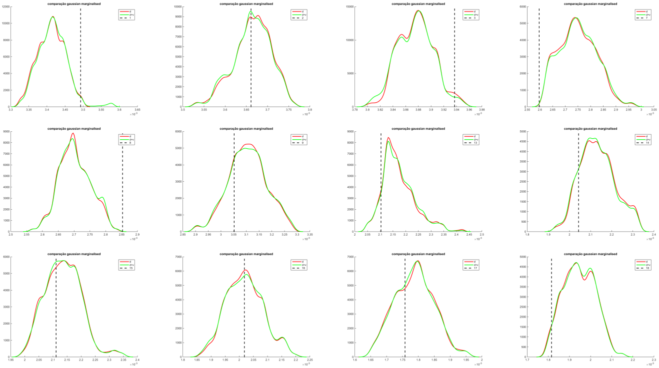

Figure: PDFs of deposition in extracted validation points $\{1, 2, 3, 7, 8, 9, 13, 14, 15, 16, 17, 18\}$ comparing with true mode

Looking into different QoIs (velocity profiles)

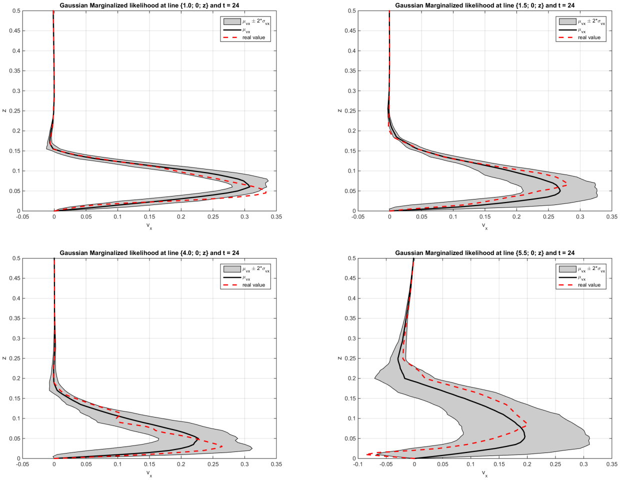

Figure: Different spatial profiles of streamwise velocity in different locations along the central line of the channel

Summarizing Calibration

The embedded model error parameter

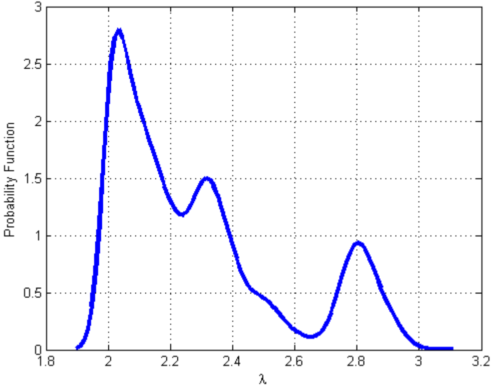

Predictive Scenarios (inlet = 0.75) : Extrapolation (t=12)

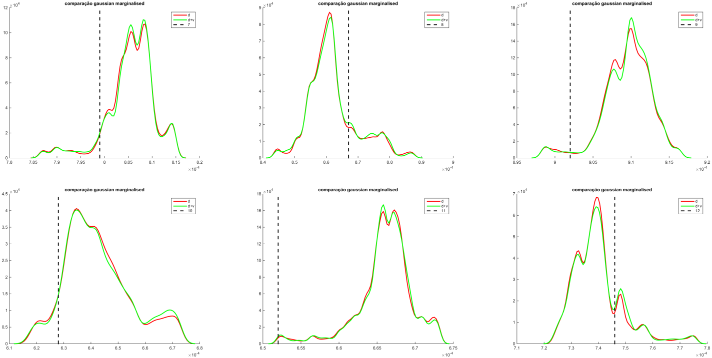

Figure: PDFs of deposition in map points compared to the solution of true model

Final Remarks and Next Steps

- We extend our RBVMS method to treat concentration-dependent viscosity and made some progress on understanding the impact of rheology on turbidity currents modeling.
- Simulations agree qualitatively with laboratory experiments observations.
- Uncertainty propagation in initial conditions and settling velocity: see Guerra et al, Computational Geosciences, 2016.
- Extending the model inadequacy idea for the settling velocity
- Integrating experimental data for enhancing prediction capabilities (Bayesian framework): model validation and calibration

Computer Simulations and Reality

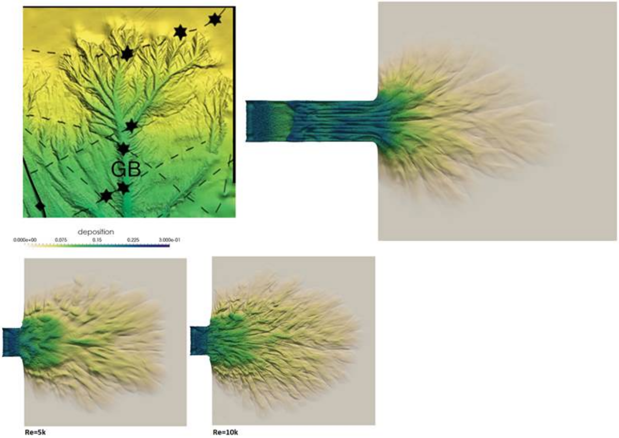

Similar patterns : Bathymetry of the Grand Banks slope